BIOCHEMICAL AND BIOPHYSICAL RESEARCH COMMUNICATIONS **219,** 191–197 (1996)
ARTICLE NO. 0204

The Solution Structure of a Psoralen Cross-Linked DNA Duplex by NMR and Relaxation Matrix Refinement

Geum-Sook Hwang,* Jong-Ki Kim,† and Byong-Seok Choi*,[1]

*Department of Chemistry, Korea Advanced Institute of Science and Technology, Taejon 305-701, Korea; and †Department of Biomedical Engineering and Radiology, Catholic University of Taegu-Hyosung, School of Medicine, Taegu 705-716, Korea

Received December 19, 1995

The three dimensional structure of the DNA oligomer d(5′-GGGTACCC-3′)$_2$ cross-linked with 4′-aminomethyl-4,5′,8-trimethylpsoralen(AMT) has been determined by two-dimensional NMR and a relaxation matrix refinement method. NMR data and structural calculation establish that the cross-linking of the psoralen in the B-DNA duplex retains Watson-Crick type hydrogen bonding throughout the duplex, although the thymine residue which is cross-linked with psoralen forms a weaker hydrogen bond. The psoralen cross-linking in DNA duplex induces significant change of the local DNA structure, but has no important effect on overall DNA helix. Our observation places an upper limit of 10° on overall DNA bending by psoralen cross-linking, which is consistent with the result of HMT-octamer cross link [Spielmann, H. P., Dwyer, T. J., Sastry, S. S., Hearst, J. E., and Wemmer, D. E., (1995) *Proc. Natl. Acad. Sci. USA* **92,** 2345–2349] and gel electrophoretic study [Haran, T. E., and Crothers, D. E. (1988) *Biochemistry* **27,** 6967–6971].

Psoralens are linear furocoumarins that photochemically alkylate nucleic acids and have been used as intercalating DNA binding drugs in the photochemotherapy of skin diseases(1-3). The photochemical reactions take place at the 3,4 or 4′,5′ double bonds of the psoralen with the 5,6 double bond in pyrimidines. The planar psoralen first intercalates into a double helical region, and ultraviolet (320-410nm UVA) irradiation initially induces a single cyclobutane addition with a pyrimidine base. The furane-side monoadduct still absorbs in this wavelength region, so that a second photoaddition can occur with the pyrone side to form the cross-link (see Figure 1) (4). Psoralen cross-linking occurs at 5′-TpA-3′ sites in DNA (5–6) and its photoproducts are primarily in the cis-syn conformation(7).

The psoralen-adducted DNA interferes with replication and transcription, and is recognized and efficiently removed by repair enzyme systems (8–12). Therefore, structural studies of the site specifically psoralen adducted DNA oligomers are required to understand relevant biological processes. A solution structure derived from NMR data for the 4′-aminomethyl-4,5′,8-trimethylpsoralen(AMT)-d(5′GGGTACCC-3′)$_2$ cross-link has been reported by Tomic et al (13). The NMR-derived model for this cross-linked oligomer indicated a 53° bend into the major grove. Likewise, theoretical model building studies based on the crystal structure of the psoralen-thymine monoadduct suggest that each cross-link bends the DNA double helix by 46.5° (14). On the other hand, gel migration assays have concluded that no significant bending of the DNA occurs at a psoralen cross-link (15,16). Also, recent data for the solution structures of the 4′-hydroxymethyl-4,5′,8-trimethylpsoralen(HMT)-d(5′-GCGTACGC-3′)$_2$ cross-link suggested that the helix axis was not bent by the psoralen cross-linking (17). Contrasting results between two NMR-derived modeling studies (13,17) may indicate the methodological limit of molecular dynamics. Therefore, detailed structural calculations are required for obtaining a more definite three-dimensional structure. Here, we have used ^{1}H NMR and full relaxation matrix refinement method to derive high

[1] To whom correspondence should be addressed. Fax: 82-42-869-2810.

Abbreviations: AMT 4′-aminomethyl-4,5′,8-trimethylpsoralen; HMT, 4′-hydroxymethyl-4,5′,8-trimethylpsoralen; NOESY, nuclear Overhauser effect spectroscopy, DQF-COSY, double quantum filtered correlated spectroscopy.

0006-291X/96 $18.00

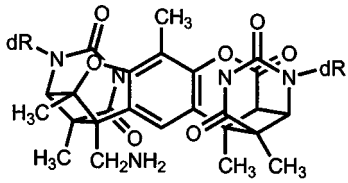

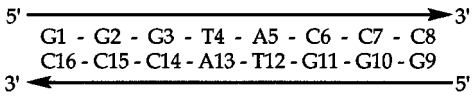

FIG. 1. The *cis-syn* AMT cross-link with thymines and DNA sequence context.

quality NMR data and a well resolved solution structure for the AMT-d(5′-GGGTACCC-3′)$_2$ cross-link (Figure 1), and to compare the AMT cross-linked DNA with the HMT cross-linked DNA.

MATERIALS AND METHODS

1. Preparation of AMT-oligomer cross-link. The DNA oligomer, d(GGGTACCC), was synthesized on an automated applied biosystems DNA synthesizer using β-cyanomethyl phosphoramidite chemistry on a 10 μmole scale and purified by gel filtration column chromatography. The purified oligonucleotides and AMT together were dissolved in 30mM Na_2HPO_4 buffer. This solution was stirred at room temperature for 1 hour under nitrogen atmosphere, and was irradiated with 350 nm UV light at 0°C for 15 minutes after stirring. This procedure was repeated with one more addition of AMT to the solution to achieve maximum yield. After irradiation, the reaction mixture was diluted with 8M urea, heated to 50–60°C in water bath, and maintained at that temperature for 10 minutes. The reaction mixture was lyophilized and resuspended in small volume, and subjected to a P-10 gel filtration column chromatography with 4M urea, 40mM CH_3COONH_4 buffer, pH 7, at a flow rate of 0.5ml/min. The fractions containing psoralen cross-linked oligomer were pooled, concentrated and dialyzed to remove urea and other contaminant, and then lyophilized to dryness. Finally, this cross-linked oligomer was dissolved in 1ml of distilled water and desalted by Sephadex G-25 column. The sample was lyophilized and redissolved in 0.5ml buffer containing 20mM sodium phosphate, 150mM sodium chloride, pH 7.

2. NMR experiment. All NMR spectra were obtained on Bruker AMX-500 MHz and DMX-600 MHz spectrometers, and the data were processed on Silicon Graphics computer using the program FELIX 2.30. The phase sensitive NOESY spectra were acquired with 60ms, 100ms 180ms, 250ms using time proportional phase incrementation(18). The spectra were acquired with 2K points in the t_2 direction and 512 points in the t_1 direction. The time-domain data were zero filled in both directions and were multiplied with $\pi/3$ shifted squared sine function before Fourier transformation. The double-quantum-filtered correlated (DQF-COSY) spectrum(19) was recorded with 5kHz, and was acquired with 4K points in the t_2 direction and 512 points in the t_1 direction. The time-domain data were zero filled in both directions and were multiplied with $\pi/6$ and $\pi/12$ shifted squared sine function in the t_2 and t_1 direction, respectively before Fourier transformation.

3. Molecular modeling and structure refinement. Simulation, using the X-PLOR (20) program installed an a Cray 270 super computer, was performed in a vacuum with a distance-dependent dielectric constant scheme. A total 305 interproton distances were constrained in the restrained molecular dynamics calculation. Atomic partial charges of AMT cross-linking octamer were reoptimized like those in the CHARMM (21) force field according to the neutral charge scheme. During the equilibration at 1000K for 5ps, the force constants for the distance restraints were scaled up gradually to 147kJ/mol. Then the productive dynamics were simulated for 20ps at 300K. The trajectories of last 6ps were averaged and the averaged coordinates were subjected to restrained energy minimization by the 500-step Powell scheme. In order to account for potential spin diffusion effects, the distance-refined structure was calculated again using full relaxation matrix refinement in X-PLOR against NOE volume intensity data which were measured at two mixing time, 100ms and 180ms. The methyl group protons were $\langle r^{-3} \rangle$-weighting averaged. During the equilibration at 400K for 1ps, the weighting factor for the intensity error were scaled up gradually to 420 kJ/mol. Then, the productive dynamecs were simulated for 10ps at 300K. The trajectories of last 3ps were averaged and the averaged coordinates were subjected to restrained energy minimization by the 30-step Powell scheme.

RESULTS AND DISCUSSION

An expanded portion of a 250-ms NOESY spectrum of the cross-linked octamer duplex in D_2O buffer solution, at 10°C, is shown in Figure 2. This contour plot outlines the sequential intrastrand

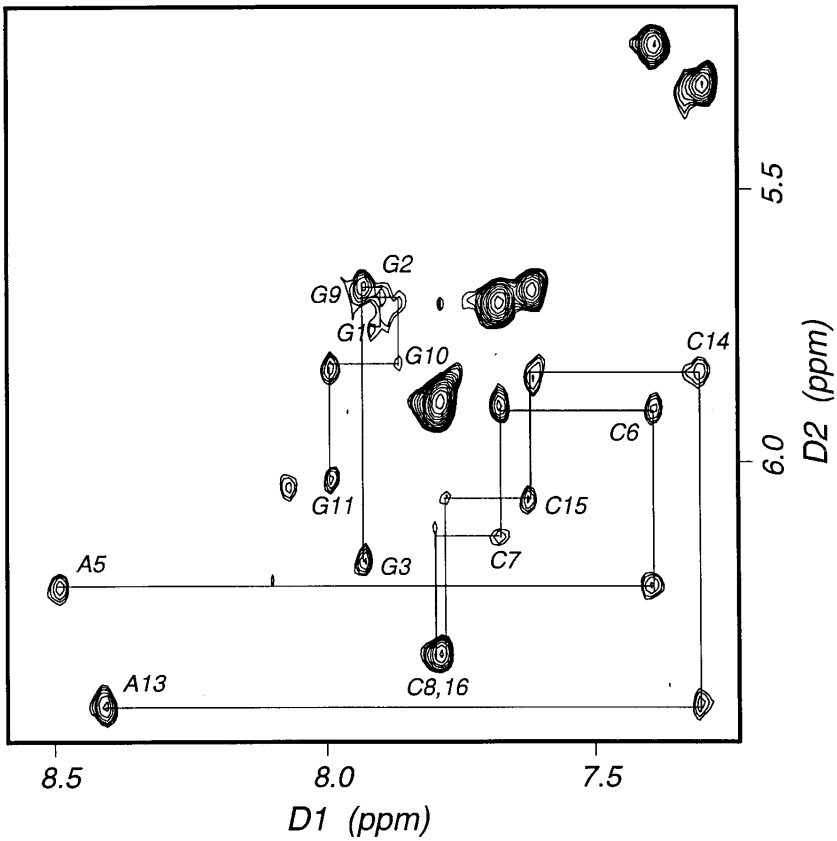

FIG. 2. Expanded NOESY(250-ms mixing time) contour plot of the AMT cross-linked octamer in 20 mM Na_2HPO_4, 150 mM NaCl D_2O, pH 7.0, 10°C. Figure shows a typical region (base protons to H1′) in the sequential NOE connectivity of the psoralen cross-linked octamer.

NOE connectivities between the base H8/H6 protons and the sugar H1′ and cytosine H5 protons. The covalently bound psoralen breaks the symmetry of the DNA so that previously equivalent protons on the two strands have separate resonances, which complicates the spectra. Sequential NOEs of the psoralen cross-linked strand, d(GGGTACCC), were regular from residue G1 to G3 and from residue A5 to C8, but were not observed at the psoralen adducted T4. Similar results were also observed in the complementary strand. The change in atomic orbital hybridization of the C5 and C6 atoms of the thymine base upon the formation of the covalent bond between thymine and psoralen leads to the large upfield shifts of the H6 protons of T4 and T12 (see Table 1). Cross-peaks between these adducted thymine H6 protons and psoralen protons indicated their close proximity and cross linking formation (see Table 2). This is also demonstrated by the cross peaks between H6 proton of T4 and pyrone side protons of psoralen, 4-CH_3 and 3-H, and between H6 proton of T12 and furane side proton, 5′-CH_3. The weak cross-peaks between the H6 proton of thymine and the H1′ proton of its 3′ adenine neighbor were observed, indicating that a AMT located directly between the A-T base pairs. The ^1H chemical shifts of the cross-linked octamer are listed in Table 1.

The structure obtained from NOE distance refinement was recalculated on the basis of NOE intensity refinement. The results of this relaxation matrix refinement revealed that many NOE distances, which were used in distance refinement, were affected by spin diffusion. The root-mean-square deviation(rmsd) of the interproton distance, used only in distance refinement, was 0.0047.

TABLE 1
^{1}H Chemical Shifts of the AMT Cross-Linked Octamer

Residue	CH_3	H2/H5	H6/H8	H1′	H2′	H2″	H3′	H4′
5′								
G1			7.91	5.73	2.58	2.73	4.89	4.22
G2			7.88	5.68	2.71	2.71	4.88	4.21
G3			7.93	6.22	2.57	2.74	5.07	4.45
T4	0.90		4.47	5.93	2.12	2.40	4.72	4.17
A5		8.05	8.49	6.23	2.74	2.96	4.48	4.28
C6		4.19	7.39	5.89	2.17	2.46	4.82	4.26
C7		5.62	7.67	6.14	2.29	2.53	4.88	4.24
C8		5.90	7.78	6.35	2.35	2.35	4.66	4.12
3′								
5′								
G9			7.93	5.68	2.57	2.71	4.88	4.42
G10			7.86	5.81	2.74	2.74	4.88	4.22
G11			7.99	6.02	2.64	2.91	5.10	4.47
T12	1.15		4.06	5.56	2.09	2.18	4.71	4.22
A13		7.84	8.41	6.45	2.96	3.06	5.05	4.24
C14		5.33	7.30	5.83	2.10	2.48	4.83	4.20
C15		5.69	7.62	6.07	2.25	2.55	4.86	4.23
C16		5.90	7.78	6.35	2.35	2.35	4.66	4.12
3′								

This increased to 0.0238 after relaxation refinement. Statistical estimation is shown in Table 3. The refined structure of the AMT cross-linked octamer duplex is shown in Figure 3. As shown in 2D spectrum of cross-linking octamer, the symmetry of NMR resonance in the unmodified octamer is broken by the cross-linking of the AMT, but the terminal residues of the cross-linking octamer are degenerated and equivalent in chemical shift, indicating that the structural disturbance upon cross linking of the AMT is limited to central four base pairs from the site of psoralen addition. As a result, NOEs from the terminal residues were not adequately used in the structure determination of the cross-linking octamer, so that terminal bases are frayed and undergoing conformational exchange. As were shown in NMR data, normal Watson-Crick hydrogen bondings were presented in the cross-linked octamer except for the thymine residues. Due to distinctive base orientation of the thymine residues upon cross-linking with AMT and steric interaction between the base of octamer and the side chain of the AMT, the hydrogen bonds of thymine residues were different from those of the unmodified octamer. In particular, the T4 residue which had large upfield shifts and broad-

TABLE 2
NOEs between DNA Oligomer Protons and Psoralen Protons

DNA				Psoralen	
Residue	Protons	δ (ppm)		Protons	δ (ppm)
T4	H6	(4.47)	↔	3-H	(1.52)
				4-CH_3	(2.47)
T4	5CH_3	(1.15)	↔	5-H	(6.51)
T12	5CH_3	(0.90)	↔	4′-CH_2	(3.58)
T12	H6	(4.06)	↔	5′-CH_3	(1.67)

TABLE 3
Structure Refinement Statistics and Analysis

Refinement	Number of distance restraints	Number of intensity restraints	rmsd of NOE distance (nm)	rmsd of Bond length (nm)	rmsd of Bond angle (degrees)	rmsd of Improper (degrees)	R-factor
Distance refinement	305	—	0.0047	0.0018	3.553	10.131	
Relaxation refinement	113	192	0.0238	0.0015	3.108	9.667	0.068

The NOE distance values are rmsd after refinement for the NOE distance constraints used only in distance refinement.

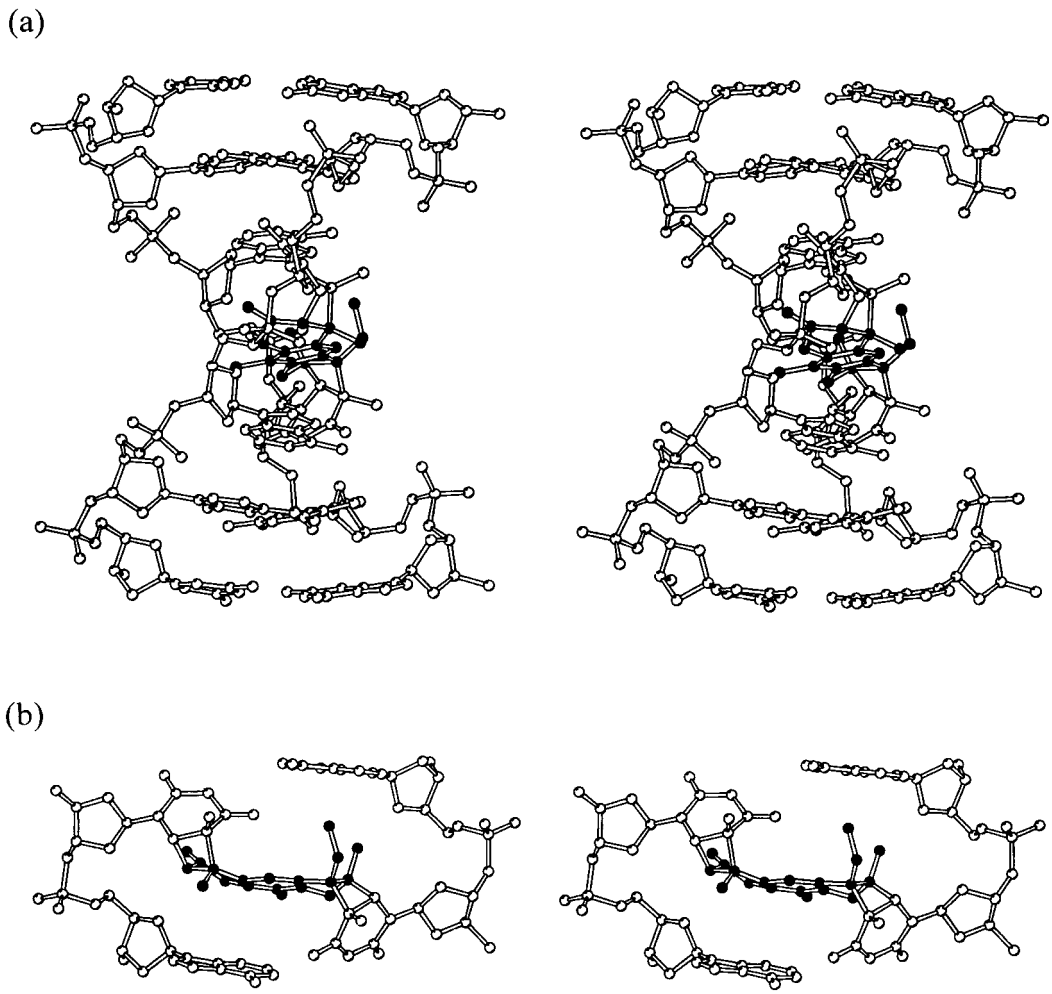

FIG. 3. Refined structure of overall helix (excluding terminal bases) (a), and its central four segments (b) of the AMT cross-linked octamer duplex, which were obtained by relaxation matrix refinement. The residue with dark-colored atoms is the AMT which is cross-linked with thymines.

ening in its hydrogen bonding sites, is rotated outside of the helix. This causes the T4 imino proton accessible to the solvent and more susceptible to exchange.

Sugar conformations of only several residues were obtained qualitatively on the basis of J-coupling constraints derived from DQF-COSY spectra, partly because of spectral overlapping and low sensitivities. The sugar rings of the flanking bases to the central four bases containing adducted psoralen were dominated by C2′-endo type conformation. The sugar conformations of the central four residues were indeterminate due to potential flexibilities of sugar rings. Therefore we did not include dihedral angle constraints explicitly in the structure refinement. In the refined structure the sugar conformations were qualitatively consistent with the observation based on J-coupling analysis. C2′-endo type were retained in the sugars of flanking bases to the central four residues. In contrast, conformational flexibilities between C2′-endo and C3′-endo were observed in the sugar residues of psoralen-adducted region.

NMR-derived structural calculations established that the AMT cross-linking in the B-DNA duplex leads to a minor bending (<10°) in the overall DNA helix. This is consistent with the recent report of the three dimensional structure of the HMT-d(5′-GCGTACGC-3′)$_2$ cross-link (17) and the earlier result of gel migration(16), but conflicts with the result of AMT-octamer cross-link by Tomic et al (13). Discrepancy between previous structure and our is due to the differential methods of the two studies. They used a starting structure in which bending was already established from molecular modeling by hand, which is usually prone to reflect user's prejudice. Distance geometry calculation was in their refinement in comparison with our molecular dynamics calculation which is much powerful in overcoming local energy minimum.

The helical axis was not kinked by cross link formation because A5 and A13 remained a nearly coplanar stack with AMT, as was the case in cross-linking with HMT. The cross-linking of psoralen in DNA duplex distorts A-T base stacking due to the structural perturbation of the thymine residue and the protrusion of the aminomethyl side chain of the psoralen. A5 residue moves slightly into the inside of helix due to a steric clash between the pyrimidine ring of the A5 and the 4-methyl group of the AMT. As a result, the hydrogen bonding of the T12 and A5 is very stable after cross-linking of AMT. In contrast, A13 residue moves into the outside of helix because aminomethylgroup extends under pyrimidine ring of A13. The G3 residue stacks onto the modified ring of the T4 and the G11 residue stacks onto the modified ring of T12. This indicates that all the residues except those in the cross-liked region are base stacked. Our results suggest overall DNA structure is largely not bent by cross linking of AMT, as was the case in HMT cross-liked DNA. Therefore, the favorable recognition by repair enzyme is probably not caused by the structural change in overall DNA helix but by the distortion of local helix structure.

ACKNOWLEDGMENTS

This work was supported by Korea Science and Engineering Foundation and Center for Molecular Catalysis.

REFERENCES

1. Cimino, G. D., Gamper, H., Isaacs, S. T., and Hearst, J. E. (1985) *Annu. Rev. Biochem.* **54,** 1151–1193.
2. Kanne, D., Straub, K., Hearst, J. E., and Rapoport, H. (1982) *J. Am. Chem. Soc.* **104,** 6754–6764.
3. Kanne, D., Straub, K., Rapoport, H., and Hearst, J. E. (1982) *Biochemistry* **21,** 861–871.
4. Isaacs, S. T., Shen, C. J., Hearst, F. E., and Rapoport, H. (1977) *Biochemistry* **16,** 1058.
5. Gamper, H., Piette, J., and Hearst, J. E. (1984) *Photochem. Photobiol.* **40,** 29.
6. Zhen, W., Buchardt, O., Nielsen, H., and Nielsen, P. E. (1986) *Biochemistry* **25,** 6598.
7. Straub, K., Kanne, D., Hearst, J. E., and Rapoport, H. (1981) *J. Am. Chem. Soc.* **103,** 2347.
8. Sancar, A., and Sancar, G. B. (1988) *Annu. Rev. Biochem.* **57,** 29–67.
9. Reardon, J. T., Spielmann, P., Huang, J.-C., Sastry, S. S., and Sancar, A. (1991) *Nucleic Acid Res.* **19,** 4623–4629.
10. Shi, Y.-B., Gamper, H., Houten, B. V., and Hearst, J. E. (1988) *J. Mol. Biol.* **199,** 277–293.
11. Sastry, S. S., and Hearst, J. E. (1991) *J. Mol. Biol.* **221,** 1091–1110.
12. Sastry, S. S., and Hearst, J. E. (1991) *J. Mol. Biol.* **221,** 1111–1125.
13. Tomic, M., Wemmer, D., and Kim, S.-H. (1985) *Science* **238,** 1722–1725.

14. Pealman, D. A., Holbrook, S. R., Pirkle, D. H., and Kim, S.-H. (1985) *Science* **227,** 1304–1308.
15. Sinden, R. R., and Hagerman, P. J. (1984) *Biochemistry* **23,** 6299–6303.
16. Haran, T. E., and Crothers, D. M. (1988) *Biochemistry* **27,** 6967–6971.
17. Spielmann, H. P., Dwyer, T. J., Sastry, S. S., Hearst, J. E., and Wemmer, D. E. (1995) *Proc. Natl. Acad. Sci. USA* **92,** 2345–2349.
18. Marion, D., and Wüthrich, K. (1983) *Biochem. Biophys. Res. Commun.* **113,** 967–974.
19. Rance, M., Sorenson, O. W., Bodenhusen, G., Wagner, G., Ernst, R. R., and Wuthrich, K. (1983) *Biochem. Biophys. Res. Commun.* **117,** 479–485.
20. Brünger, A. T. (1992) X-PLOR *Version 3.1*, Yale Univ. Press, New Haven, CT.
21. Brooks, B., Bruccoleri, R., Olafson, B., States, D., Swaminathan, S., and Karplus, M. (1983) *J. Comp. Chem.* **4,** 187–217.